Communication

Low-Dose Oxidant Toxicity and Oxidative Stress in Human Papillary Thyroid Carcinoma Cells K1

Hannah Hamada Mendonça Lens [1], Natália Medeiros Dias Lopes [1], Gabriella Pasqual-Melo [2], Poliana Camila Marinello [3], Lea Miebach [2,4], Rubens Cecchini [4], Sander Bekeschus [2,*,†] and Alessandra Lourenço Cecchini [1,5,*,†]

[1] Molecular Pathology Laboratory, Department of General Pathology, Universidade Estadual de Londrina, Londrina 86057-970, Brazil
[2] ZIK *plasmatis*, Leibniz Institute for Plasma Science and Technology (INP), Felix-Hausdorff-Str. 2, 17489 Greifswald, Germany
[3] Department of Radiation Physics, The University of Texas MD Anderson Cancer Center, Houston, TX 77030, USA
[4] Department of General, Thoracic, Vascular, and Visceral Surgery, Greifswald University Medical Center, Felix-Hausdorff-Str. 2, 17475 Greifswald, Germany
[5] Pathophysiology Laboratory of Free Radicals, Department of General Pathology, Universidade Estadual de Londrina, Londrina 86057-970, Brazil
* Correspondence: sander.bekeschus@inp-greifswald.de (S.B.); alcecchini@uel.br (A.L.C.)
† Sander Bekeschus and Alessandra Lourenço Cecchini equally contributed to this work as last authors.

Abstract: Medical gas plasmas are of emerging interest in pre-clinical oncological research. Similar to an array of first-line chemotherapeutics and physics-based therapies already approved for clinical application, plasmas target the tumor redox state by generating a variety of highly reactive species eligible for local tumor treatments. Considering internal tumors with limited accessibility, medical gas plasmas help to enrich liquids with stable, low-dose oxidants ideal for intratumoral injection and lavage. Pre-clinical investigation of such liquids in numerous tumor entities and models in vitro and in vivo provided evidence of their clinical relevance, broadening the range of patients that could benefit from medical gas plasma therapy in the future. Likewise, the application of such liquids might be promising for recurrent BRAF(V600E) papillary thyroid carcinomas, resistant to adjuvant administration of radioiodine. From a redox biology point of view, studying redox-based approaches in thyroid carcinomas is particularly interesting, as they evolve in a highly oxidative environment requiring the capability to cope with large amounts of ROS/RNS. Knowledge on their behavior under different redox conditions is scarce. The present study aimed to clarify resistance, proliferative activity, and the oxidative stress response of human papillary thyroid cancer cells K1 after exposure to plasma-oxidized DMEM (oxDMEM). Cellular responses were also evaluated when treated with different dosages of hydrogen peroxide and the RNS donor sodium nitroprusside (SNP). Our findings outline plasma-oxidized liquids as a promising approach targeting BRAF(V600E) papillary thyroid carcinomas and extend current knowledge on the susceptibility of cells to undergo ROS/RNS-induced cell death.

Keywords: BRAF; gas plasma technology; plasma medicine; ROS

1. Introduction

Thyroid carcinoma is the fifth most common cancer in women, with approximately 450,000 new cases worldwide annually [1]. The incidence is rising steadily. Covering approximately 80% of diagnosed cases, the well-differentiated papillary thyroid carcinoma (PTC) represents the most prevalent type [2]. Strikingly, although characterized by a recurrence rate of 30%, the patient's prognosis is high, given that the tumor retains expression of the thyroid sodium/iodide symporter (NIS), required for accumulation of

iodide in hormone synthesis. By that, residual or recurrent cancers are eligible for adjuvant administration of radioactive iodine. However, 40–60% of PTCs carry the oncogenic V600E mutation of the serine/threonine phosphatase BRAF, resulting in constitutive activation of mitogen-activated protein kinase (MAPK) and uncontrolled proliferation. This is of high clinical relevance as $BRAF^{V600E}$ tumors are associated with resistance to radioiodine treatment due to decreased expression of NIS, emphasizing the need of novel therapeutic approaches [3].

Lining up into an array of clinically approved redox-based therapy approaches, e.g., chemotherapeutic agents [4], photodynamic therapy [5], or radiotherapy [6], medical gas plasmas are of emerging interest in pre-clinical oncological research. Targeting the tumor redox balance, such plasmas feature a versatile mixture of reactive oxygen (ROS) and nitrogen species (RNS), causing lethal oxidative damage to cellular biomolecules [7]. Direct application of plasma-derived ROS/RNS is confined to the treatment of superficially growing, locally restricted neoplasms [8]. However, plasma-oxidized liquids can be considered concerning internal tumors with limited accessibility. Here, a carrier liquid is enriched with low-dose oxidants, applicable for intratumoral injections or lavage [9]. From a redox-chemistry point of view, only a few species are stable enough to persist in the liquid [10], and hydrogen peroxide (H_2O_2) is suggested to play a major role [11–15]. Anti-tumor effects of plasma-oxidized liquids are underlined by numerous studies, focusing on different tumor entities and a broad range of tumor models [16–21]. However, knowledge of the applicability of such an approach in the treatment of thyroid cancer is scarce. Intriguingly, besides being important from a translational point of view, characterizing ROS-based therapy approaches in thyroid carcinoma is particularly interesting, as this neoplasm evolves in a highly oxidative environment. Thyrocytes are equipped with a large amount of dual oxygenase (DUOX) 2 and NADPH-oxidase (NOX) 4, important for H_2O_2 generation required for thyroid hormone synthesis. As precise regulation of cellular H_2O_2 levels is crucial to ensure proper thyrocytes function and survival, cells are equipped with a powerful antioxidant defense system, representing an interesting target to study plasma-induced redox effects in tumor cells [22].

To this end, the present study explored metabolic activity, proliferation, viability, cellular oxidation, and the redox response of K1 cells, a lineage of papillary thyroid carcinoma carrying a heterozygous V600E mutation in the BRAF gene [23], after exposure to the plasma-oxidized medium. Cellular responses under mixed, plasma-derived ROS/RNS conditions were compared to H_2O_2 and sodium nitroprusside, an RNS donor, alone (Figure 1a). Our findings will help to understand the behavior of PTC under different redox alterations and expand to evaluate the therapeutic use of reactive species in PTC.
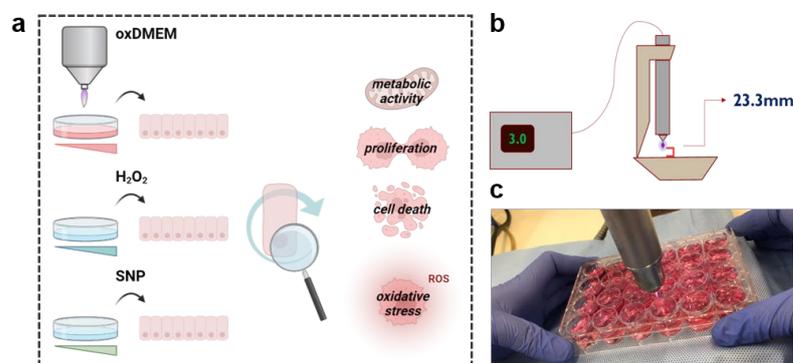

Figure 1. Study scheme and treatment procedure. (**a**) Study scheme: plasma-oxidized DMEM (oxDMEM), hydrogen peroxide (H_2O_2) and the reactive nitrogen species donor sodium nitroprusside (SNP) were investigated for their effects on metabolic activity, proliferation, viability and redox balance in a human papillary thyroid carcinoma cell line; (**b**) scheme of the generation of oxDMEM; (**c**) representative image of the generation of ox DMEM. ROS = reactive oxygen species. slm = standard liters per minute.

2. Materials and Methods

2.1. Generation of the Plasma-Oxidized Medium

The kINPen IND (neoplas, Greifswald, Germany) was used for generation of plasma-oxidized DMEM (oxDMEM) in the present study. The device is technically similar to the well-characterized kINPen Med [24]. The jet was operated with argon gas (99.999% purity) at three standard liters per minute (slm) and a effluent tip to target distance of 23.3 mm (Figure 1b). Sufficient amounts of oxDMEM were generated by exposing 1.4 mL per well of a 24-well plate to plasma for 30, 60 and 120 s (Figure 1c).

2.2. Cell Culture and Treatment Procedure

The human papillary thyroid carcinoma cell line K1 (ECACC: 92030501) was cultured in Dulbecco's Modified Eagle's Medium (DMEM):Ham's F12:MCDB 105 supplemented with 2 mM glutamine and 10% bovine fetal serum. The K1 cell line was obtained from the Cell Bank of Rio de Janeiro (Brazil), (code 0292). This human thyroid carcinoma cell line is a tetraploid subpopulation of GLAG66, and more information has been described on the Cellosaurus platform (code CVCL_2537). Cells were kept under standard culture conditions in a humidified incubator (Sanyo, Moriguchi, Japan) at 37 °C and 5% CO_2. At 24 h prior to treatment, K1 cells were seeded at a density of 2×10^5 cells per well in a 24-well flat bottom plate. The cell culture medium was removed on the day of experiment and replaced with 1 mL of oxDMEM, hydrogen peroxide (H_2O_2), or the RNS donor sodium nitroprusside (SNP) at different dosages as indicated. H_2O_2 and SNP were diluted in the fresh culture medium. For assessment of oxidant and antioxidant parameters, treatments were carried out in 25 cm^2 culture flasks, with a density of 1×10^6 cells. Likewise, cells were exposed to respective liquids for 24 h and processed as described in the following.

2.3. Cell Culture and Treatment Procedure

The MTT assay indicates the mitochondrial metabolic activity based on the ability of viable cells to convert 3-(4,5-dimethylthiazol-2yl)-2,5-diphenyl tetrazolium bromide (MTT; Sigma-Aldrich, Burlington, MA, USA) into formazan, a purple-colored crystal. At 24 h after treatment, cells were incubated with 5 mg/mL MTT for 40 min, immediately after DMSO was added, and absorbance was measured at λ_{em} = 570 nm.

2.4. Proliferation and Viability

Proliferation and cellular viability were assessed 24 h after treatment using the trypan exclusion test. Briefly, cells were detached and resuspended in 200 μL culture medium after centrifugation. Cells were stained with 0.05% Trypan blue for live–dead discrimination and counted in Neubauer chambers.

2.5. Cell Lysis

Cell lysates were prepared 24 h after treatment to assess lipid peroxidation and total radical antioxidant potential (TRAP). Briefly, 1×10^6 cells were lysed by repeated freezing in liquid nitrogen and thawing in a water bath at 30–37 °C. After three freeze–thaw cycles, lysates were centrifuged at $1000 \times g$ for 5 min at 4 °C.

2.6. Lipid Peroxidation

Oxidation of cellular membranes was assessed based on tert-butyl hydroperoxide-induced chemiluminescence, as described by Flecha and colleagues [25]. Briefly, cell homogenates were incubated with monobasic phosphate buffer (10 mM) at 37 °C for 5 min, followed by addition of hemin (1 mM) and tert-butyl hydroperoxide (6 mM). Immediately after, luminescence was measured using a luminometer (GloMax 20/20; Promega, Madison, WI, USA). Readings were performed for 20 min and 1 reading per second.

2.7. Total Radical Antioxidant Potential

Evaluation of the total radical antioxidant potential (TAR) was determined as described by [26] adapted to cells. ABAP [2,2-azo-bis (2-methylpropionamidine) dihydrochloride] was used to generate peroxyl radicals by thermal decomposition, and photon emission was amplified by addition of luminol. The amount of antioxidants present in the sample correlates with the lag time of photon emission. Briefly, glycine buffer (0.1 M, pH 8.6), ABAP solution (200 mM), and luminol (215 µM) were added to the cell lysates, and luminescence was measured immediately after using a luminometer (GloMax 20/20; Promega, Madison, WI, USA) with 5 readings per second. Trolox, a hydrosoluble vitamin E analog, was used as a standard equivalent.

2.8. Statistical Analysis

Data are from at least three independent experiments. Graphing and statistical analysis were performed using Prism 9.4.1 (GraphPad Software; San Diego, CA, USA), Excel 2007 (Microsoft, Redmond, WA, USA) and Origin 8.0 (OriginLab Software, Northampton, MA, USA). The D'Agostino and Pearson normality test was used. For parametric data ($\alpha = 0.05$), one-way or two-way analysis of variance (ANOVA) with Tukey's post hoc testing was performed, as indicated in the figure legends. The Kruskal–Wallis test with Dunn's test post hoc testing was performed on non-parametric data ($\alpha = 0.1$).

3. Results

3.1. Low-Dose Oxidants Reduce Metabolic Activity, Proliferation, and Viability in a Human Papillary Thyroid Carcinoma Cell Line

Plasma-oxidized liquids are considered promising anti-cancer tools based on their ability to target the cellular redox state via reactive species. The present study aimed to investigate responses of a human papillary thyroid carcinoma cell line K1 under different redox conditions. Besides exposure to mixed, plasma-derived ROS/RNS in plasma-oxidized DMEM (oxDMEM), metabolic activity, proliferation, viability, and redox responses were evaluated after application of H_2O_2 and SNP, an RNS donor, alone (Figure 1a). ROS/RNS composition and quantity in plasma-oxidized liquids is influenced by several factors, including feed gas and admixtures, energy supply, treatment time and also the jet-to-target distance. In the present study, the distance between effluent tip and liquid surface was 23.3 mm (corresponding to a nozzle-to-surface distance of 35 mm). The jet was operated with argon at 3 slm (Figure 1b). Sufficient amounts of plasma-oxidized DMEM were generated by exposing 1.4 mL DMEM to plasma for 30, 60, or 120 s. oxDMEM was prepared freshly before the start of experiment (Figure 1c) and added to the cells for 24 h. Exposure to oxDMEM reduced the metabolic activity of K1 cells significantly in a dose-dependent manner (Figure 2a). Similar effects were observed for H_2O_2 (Figure 2b) and SNP (Figure 2c), although high concentrations of H_2O_2 (>1 mM) in particular were needed to reduce the metabolic activity significantly. A hallmark of cancers is their sustained proliferative signaling, supported by metabolic reprogramming, ensuring supply of substrates for macromolecule synthesis. The proliferative activity of K1 cells was assessed 24 h after treatment using the trypan blue exclusion assay (Figure 3a). Again, oxDMEM reduced cellular proliferation to a significant extent in a dose-dependent manner. Similar tendencies were observed for H_2O_2 and SNP (Figure 3b). Live–dead discrimination using trypan blue staining was done to differentiate tumoristatic and tumortoxic action of the applied oxidants. At 24 h after exposure to oxDMEM, H_2O_2, or SNP, enhanced toxicity could be observed, correlating with the applied dose. Toxicity was lowest after exposure to H_2O_2 (Figure 3c).
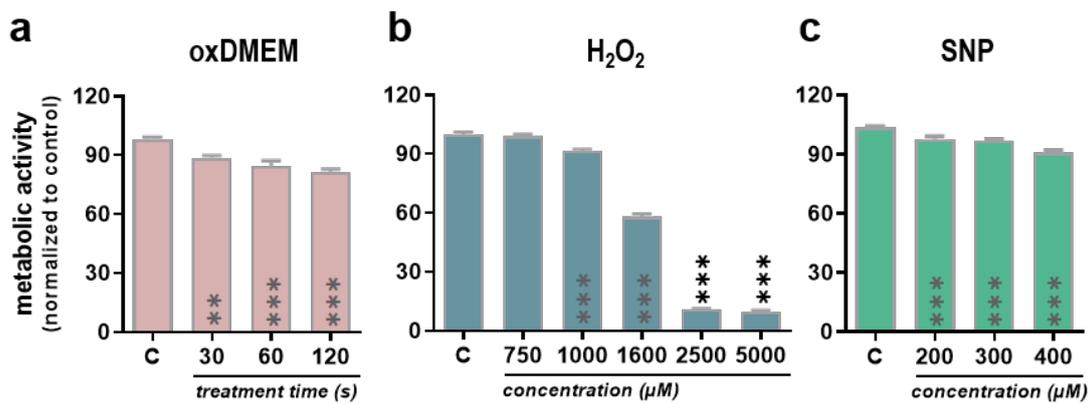
Figure 2. Metabolic activity of K1 cells after exposure to different oxidants. (**a–c**) Assessment of metabolic activity 24 h after exposure to different dosages of oxDMEM (**a**), H_2O_2 (**b**), and SNP (**c**). Bar graphs show mean ± standard error of the mean (SEM). Statistical analysis was performed using one-way analysis of variances (ANOVA) with Tukey's post hoc testing (** $p < 0.01$ and *** $p < 0.001$). C = control.
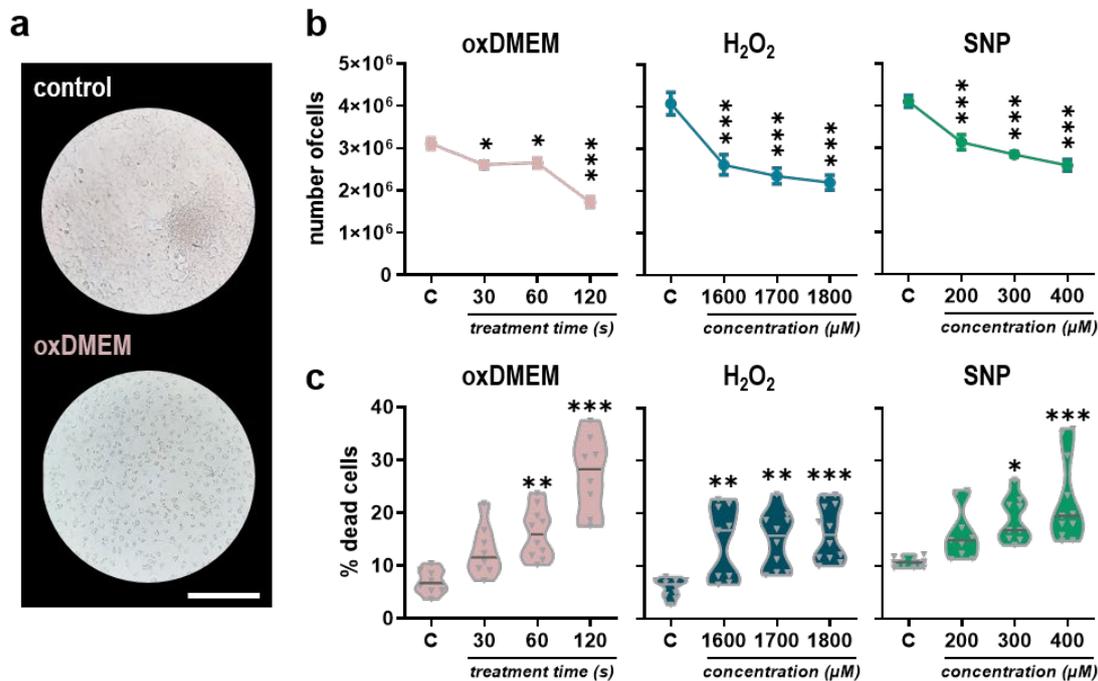

Figure 3. Proliferation and viability of K1 cells after exposure to different oxidants. (**a**) Representative *brightfield* images of K1 cells 24 h after exposure to untreated (control) or plasma-oxidized DMEM (oxDMEM); (**b**) number of cells 24 h after exposure to different dosages of oxDMEM, H_2O_2, and SNP; (**c**) percentage of dead cells 24 h after exposure to different dosages of oxDMEM, H_2O_2, and SNP. Graphs show mean ± standard error of the mean (SEM). Violin plots show median and individual values. Statistical analysis was performed using one-way analysis of variances (ANOVA) with Tukey's post hoc testing (* $p < 0.05$, ** $p < 0.01$, and *** $p < 0.001$). C = control.

3.2. Low-Dose Oxidants Induce Membrane Lipid Peroxidation without Alterations in the Antioxidant Capacity

Plasma induces cell death by irreversible damage of cellular macromolecules. A substantial impact of ROS on fatty acid chains yields cleavages and decreased membrane stiffnesses, amplifying their entry into the cells. Cellular membrane oxidation was evaluated 24 h after exposure to 60 s oxDMEM, 1800 µM H_2O_2, or 400 µM SNP in 25 cm^2 cell culture flasks. Relative detection of lipid peroxides in K1 cell lysates was done based on tert-butyl-

hydroperoxide-induced chemiluminescence [25] (Figure 4a). Overall, exposure to oxDMEM and oxidant chemicals increased lipid peroxidation in K1 cells (Figure 4b). Hereof, the increase in lipid peroxidation was highest after exposure to oxDMEM and lowest after exposure to SNP (Figure 4c). Maintaining redox hemostasis is crucial for cellular survival. Therefore, cells are equipped with a variety of enzymatic and non-enzymatic antioxidants to secure cellular macromolecules from lethal damage. In order to assess the antioxidant capacity of K1 cells after exposure to oxDMEM, the total radical antioxidant potential (TARP) was assessed 24 h after treatment (Figure 4d). Interestingly, the antioxidant capacity remained largely unchanged, with even a slight increase after exposure to 120 s oxDMEM. A significant decrease, indicative of an exhausted redox balance, was only observed after exposure to SNP (Figure 4e).
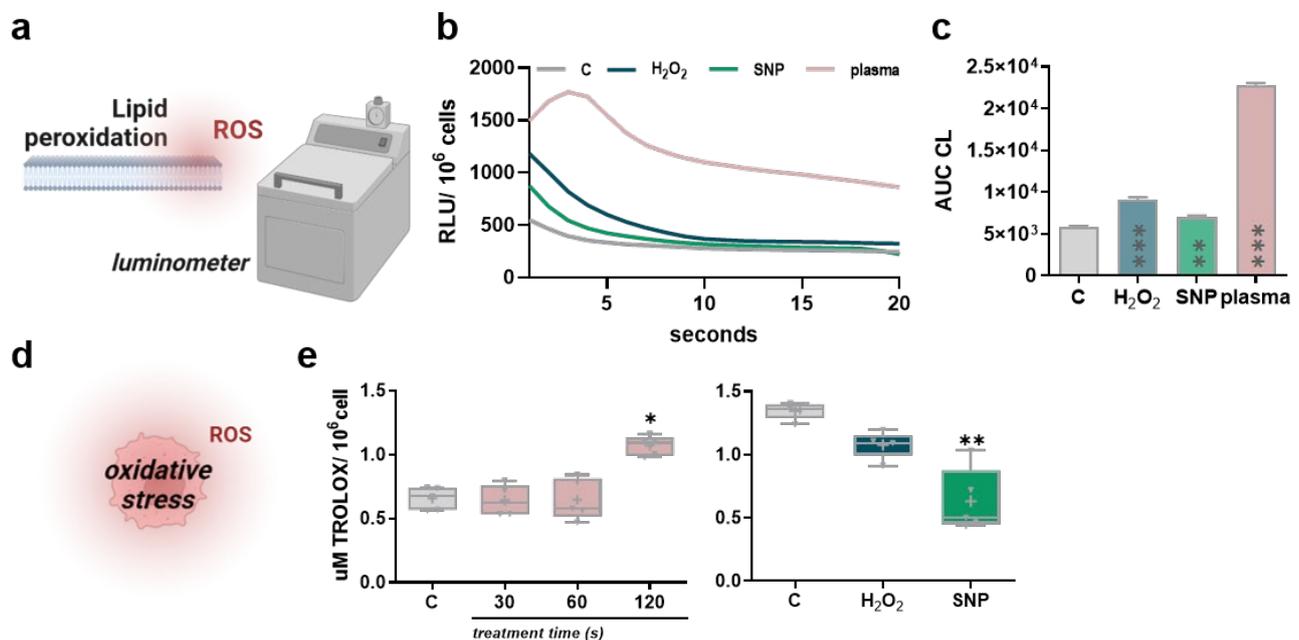

Figure 4. Lipid peroxidation and total radical antioxidant potential. (**a**) Schematic overview of chemiluminescence based assessment of cellular membrane oxidation; (**b**) relative luminescence units indicative of lipid peroxidation 24 h after exposure to 60 s oxDMEM, 1800 μM H_2O_2 and 400 μM SNP and (**c**) quantification of area under the curve; (**d**) assessment of the total radical antioxidant potential (**e**) measured 24 h after exposure to different dosages of oxDMEM, 1800 μM H_2O_2 and 400 μM SNP. Bar graphs show mean ± standard error of the mean (SEM). Box plots show median and min. to max. Mean is indicated as (+). Statistical analysis was performed using one-way analysis of variances (ANOVA) with Tukey's post hoc testing (* $p < 0.05$, ** $p < 0.01$, and *** $p < 0.001$). C = control. ROS = reactive oxygen species.

4. Discussion

Exposure to excessive amounts of ROS/RNS causes oxidative distress and irreversible damage to cells, resulting in cell death. This concept is exploited by an array of approved and emerging redox-based therapies in oncology, including medical gas plasmas. The major drawback of this promising technology is its restricted use for treatment of superficially growing, localized cancers or intraoperatively, providing better accessibility of tumors. However, the applicability of medical gas plasmas is extended upon enriching carrier solutions with gas phase-derived ROS/RNS. Plasma-oxidized liquids contain fewer but stable oxidants, applicable for intratumoral injections or lavage. Pre-clinical investigation of such liquids in numerous tumor entities and models in vitro and in vivo provided evidence of their clinical relevance, broadening the range of patients that could benefit from medical gas plasma therapy in the future [27].

Research on the applicability of medical gas plasma in treating thyroid carcinoma is still incipient. The majority of studies focused on anaplastic and medullary thyroid carcinomas and found direct plasma treatment to induce oxidative stress and apoptosis abrogated after addition of ROS/RNS scavengers [28]. In a comparative study, SNU80 anaplastic thyroid carcinoma cells were, however, found to be more resistant compared to T89G glioblastoma and KB oral carcinoma cells, with only minimal changes in antioxidant consumption after treatment pointing to their capability to cope with high amounts of ROS/RNS [29]. In 2014, Chang and colleagues provided evidence that direct application of medical gas plasmas reduces invasiveness of papillary thyroid carcinoma cells TPC-1 and BHP 10-3 via cytoskeletal alterations and decreased FAK, Src, and paxillin expression, as well as matrix metalloproteinase 2/9 and urokinase-type plasminogen activator activity [30]. Yoon and colleagues carried out pioneering research concerning the therapeutic efficacy of medical gas plasmas in the treatment of PTCs, showing enhanced toxicity and tumor immunogenicity after treatment of BCPAP PTC cells [31]. However, treatments performed in the mentioned studies were direct, which, from a clinical perspective, would only be applicable intraoperatively after thyroidectomy, to decrease recurrence rates due to micrometastases in the tumor margin. A recent study investigated transcriptional changes in a screening of five thyroid carcinoma cell lines after exposure to the plasma-oxidized medium and found plasma-induced toxicity to be associated with increased expression of GADD45, a regulator at the G2/M checkpoint playing a role in DNA damage response, cell-cycle arrest and apoptosis. The anti-tumor efficacy of the treatment was validated in a non-orthotopic model of anaplastic thyroid carcinoma in vivo [32], emphasizing the therapeutic efficacy of such an approach. The present study focused on anti-tumor effects of oxDMEM compared to H_2O_2, and the RNS donor SNP on PTC K1 cells, carrying the $BRAF^{V600E}$ mutation, being of high clinical relevance. oxDMEM affected metabolic activity, proliferation, and viability of K1 cells in a dose-dependent manner, which was associated with a significant increase in lipid peroxidation. Similar tendencies were observed after exposure to H_2O_2 and SNP, however, high concentrations were needed to elicit significant effects.

Gas plasma-oxidized liquids are considered to act mainly via H_2O_2 [33]. Important to note, thyroid tissues are capable of coping with high levels of H_2O_2, as it is essentially needed in iodide oxidation in thyroglobulin synthesis. Hence, thyroid carcinomas evolve in a highly oxidative environment, and their antioxidant defense system is naturally prepared to protect them from the high ROS levels to which they are continuously exposed [22]. For instance, the thyrocyte apical membranes exhibit low permeability of H_2O_2 into the cell [34]. Within the cells, redox homeostasis is ensured by antioxidant enzymes, including catalase, glutathione peroxidase, and glutathione reductase, as well as peroxiredoxin/thioredoxin reductase systems [35], corroborating our findings that the TARP was largely unaffected after exposure to oxDMEM and H_2O_2. In fact, recent research indicated SOD overexpression downstream *RAS* oncogene signaling to be associated with oncogenesis in thyroid carcinoma [36,37], indicating an even higher antioxidant capacity in malignant cells. However, the adaptive response of K1 cells was not enough to secure the cells from irreversible damage in the present study, as indicated by induction of cell death at high dosages.

Despite H_2O_2, plasma yields deposition of NO_2^- and NO_3^- in liquids [38]. The former is considered to act in synergy with H_2O_2, as both can form highly reactive peroxynitrites ($ONOO^-$) [39]. The present study used sodium nitroprusside as an RNS donor, a chemical compound that generates mainly nitric oxide ($NO^{\cdot}$), yielding NO_2^- and NO_3^- as secondary oxidation products [40]. In addition, $NO^{\cdot}$ itself competes for the same cytochrome oxidase c binding site as oxygen with higher affinity, inhibiting ATP production oxygen in the mitochondrial respiratory chain [41]. Furthermore, $NO^{\cdot}$ reacts with anion superoxide radical (O_2^-) in mitochondria to form $ONOO^-$. $ONOO^-$, in turn, can damage biomolecules, generate pores in the mitochondrial membrane, resulting in Ca^{2+} and depolarization of the membrane and induction of pro-apoptotic signaling [42]. The increased reactivity of $NO^{\cdot}$ likely accounts for the high efficacy of SNP in the present study, affecting

metabolic activity, proliferation, and viability of K1 cells, as well as the total antioxidant capacity of cells. However, anti-tumor effects were observed mainly at concentrations considered highly toxic in the literature [43].

Underlying mechanisms determining the susceptibility of cells to undergo plasma-induced cell death are only beginning to be understood and many studies focused on direct plasma applications, driving mainly short-lived species chemistries, so far. Despite the robustness of the antioxidant defense system, expression of membrane aquaporins [44], cholesterol content [45], and the baseline metabolic activity [46] are discussed as important factors. Overall, these findings might translate to indirect plasma treatments alike, despite conceivable differences due to the impact of long-lived oxidants. Here, a recent screening of 35 cell lines identified cell cycle-related genes to correlate with resistance toward H_2O_2 [47]. Recent studies further indicate oscillations in oxygen consumption, energy metabolism, and redox state tightly integrated in cell cycle progression [48], which might link to observed differences in the TARP of untreated thyroid carcinoma cells in the present study. The impact of redox-dependent regulatory checkpoints changes during cell cycle progression, contributing to the sensitivity of cells towards (plasma-derived) ROS/RNS.

Overall, the present study emphasizes the therapeutic applicability and efficacy of plasma-oxidized solutions in the treatment of recurrent papillary thyroid cancer. Plasma-oxidized liquids could be used in adjuvant treatment regimes administered as intratumoral injections promising for recurrent $BRAF^{V600E}$ papillary thyroid carcinomas resistant to administration of radioiodine. As a limitation, the cell culture medium was used as a carrier solution. Their complex formulations with different antioxidant capacities, discourages their use from a translational perspective [49–51]. Future studies should focus on medical-grade carrier solutions, e.g., Ringer's lactate, 0.9% sodium chloride, to study anti-tumor effects of plasma-oxidized liquids in thyroid cancer.

5. Conclusions

Targeting thyroid carcinoma with medical gas plasma-derived ROS/RNS is promising. For the first time, the present study investigated the effect of indirect plasma treatment on PTC carrying a V600E mutation in the BRAF oncogene, being of high clinical relevance. Exposure to oxDMEM showed human PTC K1 cells to be affected in metabolic activity, proliferation, viability, and redox balance highlighting its use in oncological treatment regimes in the future. Similar effects were observed after exposure to H_2O_2 and SNP, linking the impact of ROS/RNS to the observed effects.

Author Contributions: Conceptualization, S.B. and A.L.C.; methodology, A.L.C.; software, H.H.M.L., N.M.D.L. and G.P.-M.; validation, P.C.M. and L.M.; formal analysis, H.H.M.L. and L.M.; investigation, H.H.M.L., N.M.D.L., G.P.-M., P.C.M. and L.M.; resources, S.B., R.C. and A.L.C.; data curation, H.H.M.L.; writing—original draft preparation, H.H.M.L., L.M., S.B. and A.L.C.; writing—review and editing, S.B. and A.L.C.; visualization, L.M.; supervision, R.C. and A.L.C.; project administration, A.L.C.; funding acquisition, S.B. and A.L.C. All authors have read and agreed to the published version of the manuscript.

Institutional Review Board Statement: Not applicable.

Informed Consent Statement: Not applicable.

Data Availability Statement: The underlying data of this work can be retrieved from the corresponding authors upon reasonable request.

Conflicts of Interest: The authors declare no conflict of interest.

References

1. Sapuppo, G.; Tavarelli, M.; Russo, M.; Malandrino, P.; Belfiore, A.; Vigneri, R.; Pellegriti, G. Lymph node location is a risk factor for papillary thyroid cancer-related death. *J. Endocrinol. Investig.* **2018**, *41*, 1349–1353. [CrossRef] [PubMed]
2. Bongiovanni, M.; Mermod, M.; Canberk, S.; Saglietti, C.; Sykiotis, G.P.; Pusztaszeri, M.; Ragazzi, M.; Mazzucchelli, L.; Giovanella, L.; Piana, S. Columnar cell variant of papillary thyroid carcinoma: Cytomorphological characteristics of 11 cases with histological correlation and literature review. *Cancer Cytopathol.* **2017**, *125*, 389–397. [CrossRef] [PubMed]
3. Cabanillas, M.E.; McFadden, D.G.; Durante, C. Thyroid cancer. *Lancet* **2016**, *388*, 2783–2795. [CrossRef]
4. Yang, H.; Villani, R.M.; Wang, H.; Simpson, M.J.; Roberts, M.S.; Tang, M.; Liang, X. The role of cellular reactive oxygen species in cancer chemotherapy. *J. Exp. Clin. Cancer Res.* **2018**, *37*, 266. [CrossRef] [PubMed]
5. Dolmans, D.E.; Fukumura, D.; Jain, R.K. Photodynamic therapy for cancer. *Nat. Rev. Cancer* **2003**, *3*, 380–387. [CrossRef]
6. Zhang, Y.; Martin, S.G. Redox proteins and radiotherapy. *Clin. Oncol. R. Coll. Radiol.* **2014**, *26*, 289–300. [CrossRef] [PubMed]
7. Privat-Maldonado, A.; Schmidt, A.; Lin, A.; Weltmann, K.D.; Wende, K.; Bogaerts, A.; Bekeschus, S. ROS from Physical Plasmas: Redox Chemistry for Biomedical Therapy. *Oxid. Med. Cell. Longev.* **2019**, *2019*, 9062098. [CrossRef]
8. Berner, J.; Seebauer, C.; Sagwal, S.K.; Boeckmann, L.; Emmert, S.; Metelmann, H.-R.; Bekeschus, S. Medical Gas Plasma Treatment in Head and Neck Cancer—Challenges and Opportunities. *Appl. Sci.* **2020**, *10*, 1944. [CrossRef]
9. Freund, E.; Bekeschus, S. Gas Plasma-Oxidized Liquids for Cancer Treatment: Preclinical Relevance, Immuno-Oncology, and Clinical Obstacles. *IEEE Trans. Radiat. Plasma Med. Sci.* **2021**, *5*, 761–774. [CrossRef]
10. Griseti, E.; Merbahi, N.; Golzio, M. Anti-Cancer Potential of Two Plasma-Activated Liquids: Implication of Long-Lived Reactive Oxygen and Nitrogen Species. *Cancers* **2020**, *12*, 721. [CrossRef]
11. Ma, J.; Zhang, H.; Cheng, C.; Shen, J.; Bao, L.; Han, W. Contribution of hydrogen peroxide to non-thermal atmospheric pressure plasma induced A549 lung cancer cell damage. *Plasma Process. Polym.* **2017**, *14*, 1600162. [CrossRef]
12. Judee, F.; Fongia, C.; Ducommun, B.; Yousfi, M.; Lobjois, V.; Merbahi, N. Short and long time effects of low temperature Plasma Activated Media on 3D multicellular tumor spheroids. *Sci. Rep.* **2016**, *6*, 21421. [CrossRef] [PubMed]
13. Liu, J.-R.; Wu, Y.-M.; Xu, G.-M.; Gao, L.-G.; Ma, Y.; Shi, X.-M.; Zhang, G.-J. Low-temperature plasma induced melanoma apoptosis by triggering a p53/PIGs/caspase-dependent pathwayin vivoandin vitro. *J. Phys. D Appl. Phys.* **2019**, *52*, 315204. [CrossRef]
14. Matsuzaki, T.; Kano, A.; Kamiya, T.; Hara, H.; Adachi, T. Enhanced ability of plasma-activated lactated Ringer's solution to induce A549cell injury. *Arch. Biochem. Biophys.* **2018**, *656*, 19–30. [CrossRef] [PubMed]
15. Bekeschus, S.; Kolata, J.; Winterbourn, C.; Kramer, A.; Turner, R.; Weltmann, K.D.; Broker, B.; Masur, K. Hydrogen peroxide: A central player in physical plasma-induced oxidative stress in human blood cells. *Free Radic. Res.* **2014**, *48*, 542–549. [CrossRef]
16. Jezeh, M.A.; Tayebi, T.; Khani, M.R.; Niknejad, H.; Shokri, B. Direct cold atmospheric plasma and plasma-activated medium effects on breast and cervix cancer cells. *Plasma Process. Polym.* **2020**, *17*, 1900241. [CrossRef]
17. Tanaka, H.; Hosoi, Y.; Ishikawa, K.; Yoshitake, J.; Shibata, T.; Uchida, K.; Hashizume, H.; Mizuno, M.; Okazaki, Y.; Toyokuni, S.; et al. Low temperature plasma irradiation products of sodium lactate solution that induce cell death on U251SP glioblastoma cells were identified. *Sci. Rep.* **2021**, *11*, 18488. [CrossRef]
18. Liedtke, K.R.; Bekeschus, S.; Kaeding, A.; Hackbarth, C.; Kuehn, J.P.; Heidecke, C.D.; von Bernstorff, W.; von Woedtke, T.; Partecke, L.I. Non-thermal plasma-treated solution demonstrates antitumor activity against pancreatic cancer cells in vitro and in vivo. *Sci. Rep.* **2017**, *7*, 8319. [CrossRef]
19. Freund, E.; Liedtke, K.R.; van der Linde, J.; Metelmann, H.R.; Heidecke, C.D.; Partecke, L.I.; Bekeschus, S. Physical plasma-treated saline promotes an immunogenic phenotype in CT26 colon cancer cells in vitro and in vivo. *Sci. Rep.* **2019**, *9*, 634. [CrossRef]
20. Mateu-Sanz, M.; Tornin, J.; Brulin, B.; Khlyustova, A.; Ginebra, M.P.; Layrolle, P.; Canal, C. Cold Plasma-Treated Ringer's Saline: A Weapon to Target Osteosarcoma. *Cancers* **2020**, *12*, 227. [CrossRef]
21. Azzariti, A.; Iacobazzi, R.M.; Di Fonte, R.; Porcelli, L.; Gristina, R.; Favia, P.; Fracassi, F.; Trizio, I.; Silvestris, N.; Guida, G.; et al. Plasma-activated medium triggers cell death and the presentation of immune activating danger signals in melanoma and pancreatic cancer cells. *Sci. Rep.* **2019**, *9*, 4099. [CrossRef] [PubMed]
22. Ohye, H.; Sugawara, M. Dual oxidase, hydrogen peroxide and thyroid diseases. *Exp. Biol. Med.* **2010**, *235*, 424–433. [CrossRef]
23. Ribeiro, F.R.; Meireles, A.M.; Rocha, A.S.; Teixeira, M.R. Conventional and molecular cytogenetics of human non-medullary thyroid carcinoma: Characterization of eight cell line models and review of the literature on clinical samples. *BMC Cancer* **2008**, *8*, 371. [CrossRef] [PubMed]
24. Reuter, S.; von Woedtke, T.; Weltmann, K.D. The kINPen-a review on physics and chemistry of the atmospheric pressure plasma jet and its applications. *J. Phys. D: Appl. Phys.* **2018**, *51*, 233001. [CrossRef]
25. Flecha, B.G.; Llesuy, S.; Boveris, A. Hydroperoxide-Initiated Chemiluminescence—An Assay for Oxidative Stress in Biopsies of Heart, Liver, and Muscle. *Free Radic. Biol. Med.* **1991**, *10*, 93–100. [CrossRef]
26. Repetto, M.; Reides, C.; Gomez Carretero, M.L.; Costa, M.; Griemberg, G.; Llesuy, S. Oxidative stress in blood of HIV infected patients. *Clin. Chim. Acta* **1996**, *255*, 107–117. [CrossRef]
27. Tanaka, H.; Laroussi, M.; Bekeschus, S.; Yan, D.; Hori, M.; Keidar, M. Plasma-Activated Solution in Cancer Treatment. In *Plasma Cancer Therapy*; Keidar, M., Ed.; Springer: Cham, Switzerland, 2020; pp. 143–168. [CrossRef]
28. Lee, S.Y.; Kang, S.U.; Kim, K.I.; Kang, S.; Shin, Y.S.; Chang, J.W.; Yang, S.S.; Lee, K.; Lee, J.S.; Moon, E.; et al. Nonthermal plasma induces apoptosis in ATC cells: Involvement of JNK and p38 MAPK-dependent ROS. *Yonsei Med. J.* **2014**, *55*, 1640–1647. [CrossRef]

29. Kaushik, N.K.; Kaushik, N.; Park, D.; Choi, E.H. Altered antioxidant system stimulates dielectric barrier discharge plasma-induced cell death for solid tumor cell treatment. *PLoS ONE* **2014**, *9*, e103349. [CrossRef]

30. Chang, J.W.; Kang, S.U.; Shin, Y.S.; Kim, K.I.; Seo, S.J.; Yang, S.S.; Lee, J.S.; Moon, E.; Lee, K.; Kim, C.H. Non-thermal atmospheric pressure plasma inhibits thyroid papillary cancer cell invasion via cytoskeletal modulation, altered MMP-2/-9/uPA activity. *PLoS ONE* **2014**, *9*, e92198. [CrossRef]

31. Yoon, Y.; Ku, B.; Lee, K.; Jung, Y.J.; Baek, S.J. Cold Atmospheric Plasma Induces HMGB1 Expression in Cancer Cells. *Anticancer Res.* **2019**, *39*, 2405–2413. [CrossRef]

32. Jung, S.N.; Oh, C.; Chang, J.W.; Liu, L.; Lim, M.A.; Jin, Y.L.; Piao, Y.; Kim, H.J.; Won, H.R.; Lee, S.E.; et al. EGR1/GADD45alpha Activation by ROS of Non-Thermal Plasma Mediates Cell Death in Thyroid Carcinoma. *Cancers* **2021**, *13*, 351. [CrossRef] [PubMed]

33. Miebach, L.; Freund, E.; Clemen, R.; Kersting, S.; Partecke, L.-I.; Bekeschus, S. Gas plasma–oxidized sodium chloride acts via hydrogen peroxide in a model of peritoneal carcinomatosis. *Proc. Natl. Acad. Sci. USA* **2022**, *119*, e2200708119. [CrossRef] [PubMed]

34. Ekholm, R. Iodination of thyroglobulin. An intracellular or extracellular process? *Mol. Cell Endocrinol.* **1981**, *24*, 141–163. [CrossRef]

35. Bjorkman, U.; Ekholm, R. Hydrogen peroxide degradation and glutathione peroxidase activity in cultures of thyroid cells. *Mol. Cell Endocrinol.* **1995**, *111*, 99–107. [CrossRef]

36. Laatikainen, L.E.; Castellone, M.D.; Hebrant, A.; Hoste, C.; Cantisani, M.C.; Laurila, J.P.; Salvatore, G.; Salerno, P.; Basolo, F.; Nasman, J.; et al. Extracellular superoxide dismutase is a thyroid differentiation marker down-regulated in cancer. *Endocr. Relat. Cancer* **2010**, *17*, 785–796. [CrossRef] [PubMed]

37. Cammarota, F.; de Vita, G.; Salvatore, M.; Laukkanen, M.O. Ras oncogene-mediated progressive silencing of extracellular superoxide dismutase in tumorigenesis. *Biomed. Res. Int.* **2015**, *2015*, 780409. [CrossRef] [PubMed]

38. Clemen, R.; Freund, E.; Mrochen, D.; Miebach, L.; Schmidt, A.; Rauch, B.H.; Lackmann, J.W.; Martens, U.; Wende, K.; Lalk, M.; et al. Gas Plasma Technology Augments Ovalbumin Immunogenicity and OT-II T Cell Activation Conferring Tumor Protection in Mice. *Adv. Sci.* **2021**, *8*, 2003395. [CrossRef]

39. Bauer, G. The synergistic effect between hydrogen peroxide and nitrite, two long-lived molecular species from cold atmospheric plasma, triggers tumor cells to induce their own cell death. *Redox Biol.* **2019**, *26*, 101291. [CrossRef]

40. Ranadive, S.M.; Eugene, A.R.; Dillon, G.; Nicholson, W.T.; Joyner, M.J. Comparison of the vasodilatory effects of sodium nitroprusside vs. nitroglycerin. *J. Appl. Physiol. (1985)* **2017**, *123*, 402–406. [CrossRef]

41. Mason, M.G.; Nicholls, P.; Wilson, M.T.; Cooper, C.E. Nitric oxide inhibition of respiration involves both competitive (heme) and noncompetitive (copper) binding to cytochrome c oxidase. *Proc. Natl. Acad. Sci. USA* **2006**, *103*, 708–713. [CrossRef]

42. Poderoso, J.J.; Helfenberger, K.; Poderoso, C. The effect of nitric oxide on mitochondrial respiration. *Nitric Oxide* **2019**, *88*, 61–72. [CrossRef] [PubMed]

43. Varga, J.; Bator, J.; Nadasdi, G.; Arvai, Z.; Schipp, R.; Szeberenyi, J. Partial Protection of PC12 Cells from Cellular Stress by Low-Dose Sodium Nitroprusside Pre-treatment. *Cell Mol. Neurobiol.* **2016**, *36*, 1161–1168. [CrossRef] [PubMed]

44. Bienert, G.P.; Chaumont, F. Aquaporin-facilitated transmembrane diffusion of hydrogen peroxide. *Biochim. Biophys. Acta* **2014**, *1840*, 1596–1604. [CrossRef] [PubMed]

45. Van der Paal, J.; Neyts, E.C.; Verlackt, C.C.W.; Bogaerts, A. Effect of lipid peroxidation on membrane permeability of cancer and normal cells subjected to oxidative stress. *Chem. Sci.* **2016**, *7*, 489–498. [CrossRef]

46. Bekeschus, S.; Liebelt, G.; Menz, J.; Berner, J.; Sagwal, S.K.; Wende, K.; Weltmann, K.D.; Boeckmann, L.; von Woedtke, T.; Metelmann, H.R.; et al. Tumor cell metabolism correlates with resistance to gas plasma treatment: The evaluation of three dogmas. *Free Radic. Biol. Med.* **2021**, *167*, 12–28. [CrossRef]

47. Bekeschus, S.; Liebelt, G.; Menz, J.; Singer, D.; Wende, K.; Schmidt, A. Cell cycle-related genes associate with sensitivity to hydrogen peroxide-induced toxicity. *Redox Biol.* **2022**, *50*, 102234. [CrossRef]

48. Burhans, W.C.; Heintz, N.H. The cell cycle is a redox cycle: Linking phase-specific targets to cell fate. *Free Radic. Biol. Med.* **2009**, *47*, 1282–1293. [CrossRef]

49. Wende, K.; Reuter, S.; von Woedtke, T.; Weltmann, K.D.; Masur, K. Redox-Based Assay for Assessment of Biological Impact of Plasma Treatment. *Plasma Process. Polym.* **2014**, *11*, 655–663. [CrossRef]

50. Adachi, T.; Tanaka, H.; Nonomura, S.; Hara, H.; Kondo, S.; Hori, M. Plasma-activated medium induces A549 cell injury via a spiral apoptotic cascade involving the mitochondrial-nuclear network. *Free Radic. Biol. Med.* **2015**, *79*, 28–44. [CrossRef]

51. Bekeschus, S.; Kading, A.; Schroder, T.; Wende, K.; Hackbarth, C.; Liedtke, K.R.; van der Linde, J.; von Woedtke, T.; Heidecke, C.D.; Partecke, L.I. Cold Physical Plasma-Treated Buffered Saline Solution as Effective Agent Against Pancreatic Cancer Cells. *Anticancer Agen. Med. Chem.* **2018**, *18*, 824–831. [CrossRef]